derivative, and therefore the technique can be used as a sensitive probe of the thermodynamics of a quantum gas.

Our quasi-1D Bose gases are produced using ^{87}Rb atoms in the hyperfine state $|F = 2, m = 2\rangle$. A very elongated Ioffe magnetic trap with a longitudinal oscillation frequency ranging from 5.0 to 8 Hz and a transverse oscillation frequency $\omega_\perp/2\pi$ ranging from 3 to 4 kHz is realized using on-chip microwires and an external homogeneous magnetic field. Using rf evaporation, we produce ultracold clouds at temperatures from $T = 20$ to 500 nK. The longitudinal rms size L of the cloud ranges from $\sim$50 to $\sim$100 μm. Under these conditions such gases explore the crossover from the ideal gas regime to the quasicondensate regime [4], and the underlying physics lies in the 1D regime or in the crossover from 1D to 3D [6].

In situ measurements of density fluctuations are performed using absorption images such as the one shown in Fig. 1(b). The details of our imaging and calibration techniques are described in the supplementary material [13]. As the transverse size of the trapped cloud (< 500 nm rms) is much smaller than the pixel size (4.5 μm), the only information in the transverse direction is the diffractional and motional blur on the image. By summing the atom number over transverse pixels, we reduce the notion of a pixel to a segment of length Δ and derive from each image the longitudinal density profile [Fig. 1(c)]. We perform a statistical analysis of hundreds of images taken under the same experimental conditions [4,6]. For each profile and pixel we extract $\delta N = N - \langle N\rangle$, where $\langle N\rangle$ is given by the average density profile. To remove the effect of shot-to-shot variations in the total atom number $N_{\rm tot}$, the profiles are ordered according to $N_{\rm tot}$ and we use a running average of about 20 profiles. As will be explained below, the longitudinal confining potential is irrelevant and each δN is binned according to the corresponding mean atom number in the pixel $\langle N\rangle$. For each bin, we compute the second and third moment of atom number fluctuations, $\langle \delta N^2\rangle$ and $\langle \delta N^3\rangle$. The contribution of the optical shot noise to these quantities is subtracted, although it is negligible for $\langle \delta N^3\rangle$.

The measured third moment of the atom number fluctuations, $\langle \delta N^3\rangle_m$, is plotted in Fig. 2 for two different temperatures. For the higher temperature [Fig. 2(a)], we observe a positive value of $\langle \delta N^3\rangle_m$ that increases with $\langle N\rangle$. At a smaller temperature [Fig. 2(b)], $\langle \delta N^3\rangle_m$ initially grows with $\langle N\rangle$ and reaches a maximum, before taking a value compatible with zero at large $\langle N\rangle$. The corresponding second moments or variances $\langle \delta N^2\rangle_m$ are shown in the insets. A finite third moment indicates an asymmetry of the atom number distribution, which is usually quantified by the skewness $s_m = \langle \delta N^3\rangle_m/\langle \delta N^2\rangle_m^{3/2}$, shown in Figs. 2(c) and 2(d). Before discussing the physics behind these results, we first describe how the *measured* moments $\langle \delta N^3\rangle_m$ and $\langle \delta N^2\rangle_m$ are related to the *true* moments $\langle \delta N^3\rangle$ and $\langle \delta N^2\rangle$.

The measurements of atom number fluctuations are affected by the finite spatial resolution due to both the optical resolution and the diffusion of atoms during the optical pulse, which cause the absorption signal from each atom to spread over several pixels and blur the image. Denoting by $\mathcal{A}$ the impulse response function of the imaging system, the impulse response for the pixel $[0, \Delta]$ is $\mathcal{F}(z_0) = \int_0^\Delta dz \mathcal{A}(z - z_0)$, and the measured atom number fluctuation in the pixel is given by $\delta N_m = \int_{-\infty}^{+\infty} dz_0 \mathcal{F}(z_0)\delta n(z_0)$, where $\delta n(z_0)$ is the local density fluctuation. For the parameters explored in this Letter, the expected correlation length l_c of density fluctuations [14] is smaller than 0.5 μm. This is sufficiently smaller than the width of $\mathcal{A}$ so that we can assume that the density fluctuations have zero range. Moreover, since the resolution and the pixel size are much smaller than the longitudinal size of the cloud, we can assume that the gas is locally homogeneous with respect to z. Then, the measured second and third moments can be obtained as

$$\langle \delta N^2\rangle_m = \langle \delta N^2\rangle \int_{-\infty}^{+\infty} dz_0 \mathcal{F}(z_0)^2/\Delta = \kappa_2 \langle \delta N^2\rangle, \quad (1)$$

$$\langle \delta N^3\rangle_m = \langle \delta N^3\rangle \int_{-\infty}^{+\infty} dz_0 \mathcal{F}(z_0)^3/\Delta = \kappa_3 \langle \delta N^3\rangle, \quad (2)$$

where $\langle \delta N^2\rangle$ and $\langle \delta N^3\rangle$ are the respective true moments, whereas κ_2 and κ_3 are the reduction factors. For low enough linear densities, the gas lies in the nondegenerate ideal gas regime. Then the fluctuations are almost that of a Poissonian distribution, so that $\langle \delta N^2\rangle \simeq \langle \delta N^3\rangle \simeq \langle N\rangle$, and the reduction factors may be deduced from a linear fit of the measured fluctuations versus $\langle N\rangle$, where $\langle N\rangle$ is experimentally determined absolutely. However, such a

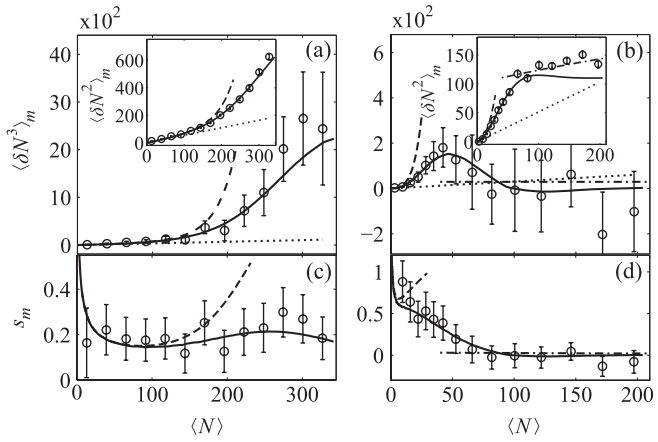

FIG. 2. Measured third moment (open circles) of the atom number fluctuations versus the mean atom number per pixel, for temperatures of 376 nK (a) and 96 nK (b). The insets show the corresponding atom number variances. The error bars are the statistical errors. Graphs (c) and (d) show the skewness s_m corresponding to (a) and (b), respectively. The theoretical predictions, scaled by $\kappa_2 = 0.55$ and $\kappa_3 = 0.34$ for (a) and (c), and by $\kappa_2 = 0.52$ and $\kappa_3 = 0.31$ for (b) and (d), are shown for comparison: solid lines, the modified Yang-Yang prediction; dashed lines, the ideal Bose-gas prediction; dash-dotted lines on (b) and (d), the quasicondensate prediction; dotted lines, the shot-noise limit $\langle N\rangle$.